

COMPARISON OF VORTICAL STRUCTURES OF A HELICOPTER ROTOR MODEL MEASURED BY LDV AND PIV

U. Seelhorst, M. Raffel, C. Willert, H. Vollmers, K.A. Bütetisch, J. Kompenhans

Institut für Strömungsmechanik
Deutsche Forschungsanstalt für Luft- und Raumfahrt (DLR)
Bunsenstr. 10, D-37073 Göttingen, Germany

Abstract

Flow field measurements of the blade tip vortices at a rotating helicopter rotor model were performed by three component laser-Doppler velocimetry (3D-LDV) and conventional (two component) particle image velocimetry (PIV). The results are in good correspondence in general, but also illustrate the different properties of both techniques, such as the three-dimensional measurement capability of LDV and the unsteadiness of the flow captured by the PIV method.

Introduction

With increasing use of civil helicopters the problem of noise emission of helicopters has become increasingly important within the last decades. Helicopter noise has been subject of many research projects (Lowson 1991). Blade vortex interactions (BVI) have been identified as a major source of impulsive noise. As BVI-noise is governed by the induced velocities of tip vortices, it depends on vortex strength and miss-distance, which itself depends on vortex location, orientation, and convection speed relative to the path of the advancing blade. Blade vortex interaction can occur at different locations inside the rotor plane depending on flight velocity and orientation of the blade tip path plane. It has to be distinguished between parallel blade vortex interaction, the angle between leading edge of the blade and vortex axis is about 0° , and orthogonal blade vortex interaction, where the angle between leading edge and vortex axis is close to 90° . The noise emission of parallel blade vortex interaction is considerably larger (Cardonne et al. 1988, Spletstößer et al. 1990). Investigations of the acoustic near and farfield (Ehrenfried et al. 1991, Burley et al. 1991) were based on the interaction of the blade with vortices, which were described by mathematical models. Information about the structure and strength of the real rotor tip vortices and their interaction with the blade were not available. It is understood, that the study of these phenomena is of particular interest for progress towards quieter helicopters.

In our investigations the vortical structures of the flow field of helicopter rotor model in a wind tunnel has been studied by optical measurement techniques, since only non-intrusive techniques are capable to obtain velocity data within the rotor plane. Measurements of local flow vectors at positions close to the rotor blade tips were performed by three component laser Doppler velocimetry

(3D-LDV) and conventional (two component) particle image velocimetry (PIV). For the first time a comparison of LDV and PIV data acquired in a wind tunnel from the same rotor model has been performed. The blade position has to be chosen where vortex positions and their orthogonal interactions with the blade are well known and easily reproducible (see Fig. 1, position B).

Rotor and test matrix

The LDV and PIV measurements have been performed on the helicopter rotor model of the Department of Aerospace Engineering (ILR) of RWTH Aachen, developed and investigated in detail by Beesten (1994). The rotor model had a radius of 0.5 m and four NACA 0015 blades (chord length = 54 mm) with rectangular tips and was driven by a toothed belt and an electric 65 kW engine. The rotor model was fully articulated and had flapping hinges. The rotor was installed in the open test section of the ILR Aachen low-speed wind tunnel.

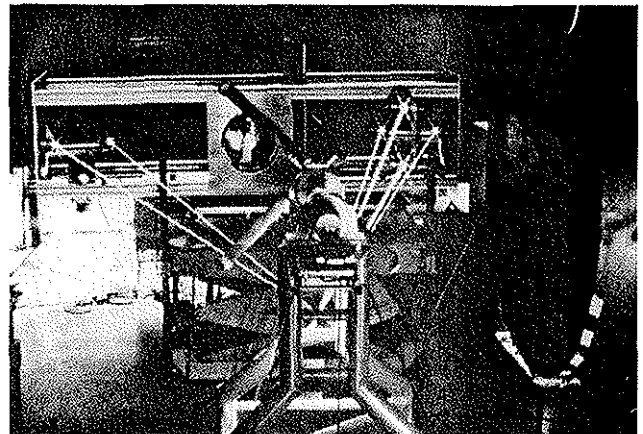


Figure 1: 3D-LDV and helicopter rotor model in the open test section of the ILR Aachen low-speed wind tunnel.

The free stream velocity was set to $U = 15.7$ m/s and the rotor speed to $f = 25$ rev/s resulting in an advance ratio of $\mu \approx 0.2$. The tip path plane was tilted by an angle of $\alpha_{TPP} = -3^\circ$ against the mean flow (forward flight), the collective part of the angle of attack was $\nu_{coll} = 10^\circ$, and the cyclic pitch was $\nu_{cycl} = \pm 3.5^\circ$ resulting in trimmed condition. The Reynolds number, based on the main chord length and blade tip velocity, was $Re \approx 278.000$.

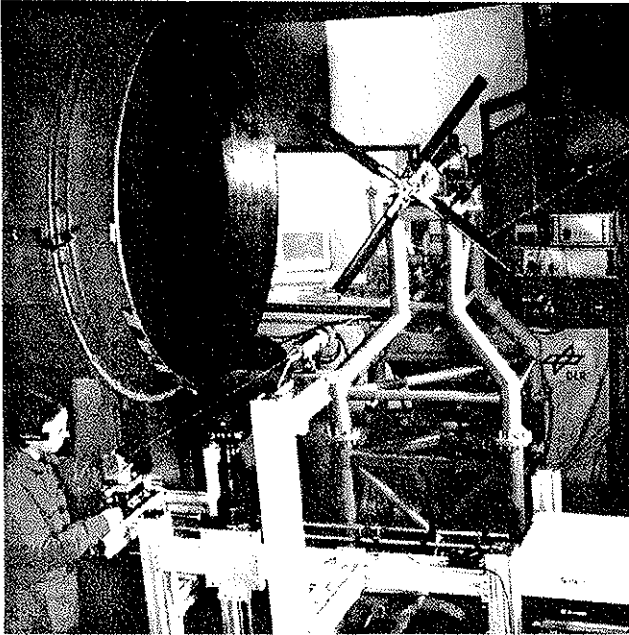


Figure 2: PIV set-up and helicopter rotor model in the open test section of the ILR Aachen low-speed wind tunnel.

For the investigation of the blade tip vortex itself 3D-LDV measurements have been performed at an azimuth angle of $\psi \approx 0^\circ$ in a plane outside the rotor (see Fig. 3, position A). At this position the blade tip vortex, generated at $\psi = 0^\circ$, is about 3 ms old and has rolled up completely so that there is no temporal change in the vortex structure itself. The blade load, and therefore the vortex strength is at this azimuthal position similar to that at $\psi = 90^\circ$.

For the investigation of orthogonal blade vortex interaction LDV and PIV measurements have been taken at an azimuth angle of $\psi \approx 90^\circ$ (advancing blade side) in a plane perpendicular to the free stream velocity (see Fig. 3, position B).

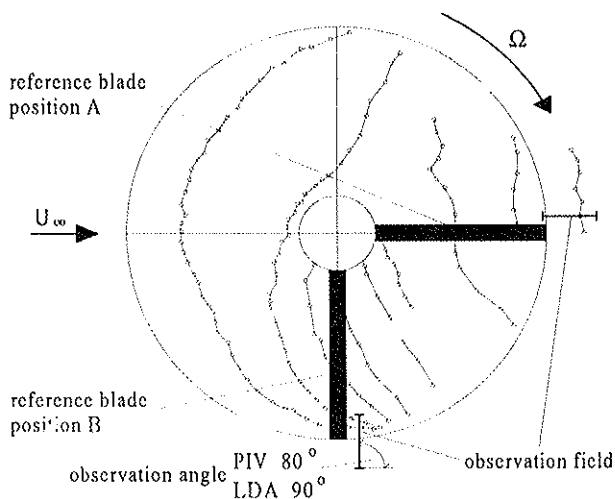


Figure 3: Sketch of the paths of the tip vortices at an advance ratio of $\mu = 0.2$, viewing direction parallel to the rotor axis, according to Beesten (1994) - not to scale.

3D-LDV set-up

The new 3D-LDV of the DLR Institute for Fluid Mechanics brought major improvements concerning sensitivity, data rate and the resolution of the insight velocity component (Seelhorst et al. 1993). As can be seen in Figure 4, the system was operated in a back scatter, off-axis mode. A 6 Watt argon-ion laser was used as a light source of which the three most intensive laser lines (476.5 nm, 488 nm, 514.5 nm) were utilized to distinguish the different velocity components. Each of the laser beams was divided into two individual beams with similar intensity, one superimposed with a Bragg shift of 40 Mhz for ambiguity removal. The beams were coupled into single mode glass fibres and were launched into the probe volume with individual transmitting optics. In order to provide a good resolution of the insight velocity component the angle between the optical axes was set to 30° . The effective size of the probe volume was approximately 0.25 mm in diameter and 1 mm in length. The tracer particles used were the same for both the LDV and PIV measurements: oil droplets, with an average diameter of less than $1 \mu\text{m}$. As the receiving optics of the system operated in back-scatter mode, a sufficiently high data rate requires the f-number of the receiving optics to be as small as possible. In this case a modified Schmidt-Cassegrain telescope with an aperture of 350 mm ($f = 12$) was used in order to gather enough scattered light from the particles. The received light, containing information of all three velocity components, was coupled into a multi-mode glass fibre, which transmitted the light to a prism system, in order to separate the different wavelengths. Then the light was converted into an electrical signal by three separate photo-multipliers.

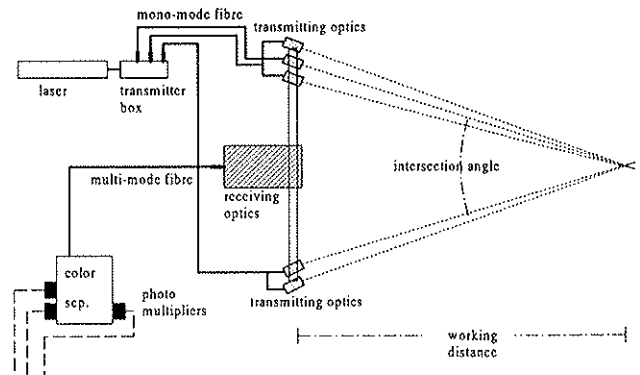


Figure 4: Sketch of the 3D-LDV system.

After digitization of the signals a fast Fourier analysis yielded the desired Doppler frequency. Only if the signals of the three components coincided the velocity data was stored together with the actual time and measuring position.

Based on the assumption of a periodic flow field with respect to the rotor revolution, conditional sampling was used to get time dependent information of the flow field. A trigger signal from the rotor axis was shifted with a time

delay to any preselected azimuthal position of the rotor blade with an accuracy of 0.3% with respect to the rotor revolution. At this position the clock of the data acquisition system was set to zero. Data acquisition was then started for a time window, corresponding to an azimuthal window or a time interval needed for the flow structure to pass through the probe volume. Usually data were acquired just within a small azimuthal window of 20° to 60°.

Converting time information into spatial information can be done in different ways. In this case the transformation of the time information into an equivalent azimuthal angle was done by the following equation:

$$\Psi = \Psi_0 + 2\pi \cdot f \cdot t, \text{ where } f \text{ is the rotor frequency.}$$

The transformation of the time dependent information into a spatial information of the flow structure as for example the length l was done by analysing the convection speed of the flow structure:

$$l = U_{conv} \cdot t.$$

Using the conditional sampling mode to acquire time resolved velocity data, which is later converted into spatial velocity data, leads to an inaccuracy due to the fact that flow structures may change during the time interval t , corresponding to the equivalent azimuthal angle. This has to be balanced against the significant reduction of measuring time.

A 'position monitoring system' gave access to blade motion parameters (lead-lag motion, pitching motion and angle of incidence) at a preselected radial position of the blade.

PIV recording system

During the last decade PIV has increasingly been used to measure instantaneous flow velocity fields. This technique, in contrast to LDV, requires no conditional sampling. PIV allows to capture the flow velocity in a two-dimensional plane of the flow within a few microseconds. It therefore enables to obtain data of the entire velocity field even in case of large cycle-to-cycle variations. The fact, that the recording time, necessary for the application of PIV ($\approx 12 \mu\text{s}$), is small compared to the time required for one revolution cycle ($\approx 40.000 \mu\text{s}$) makes PIV an ideal tool for the investigation of the unsteady flow fields associated with rotor aerodynamics.

During the last years a PIV system has been developed at DLR which can be operated under rough environmental conditions in wind tunnels (Kompenhans et al. 1994). This system utilizes a two-oscillator Nd:YAG pulse laser system with a pulse energy of $2 \times 70 \text{ mJ}$ for illumination of an area of up to $20 \times 30 \text{ cm}^2$ of the flow field. The recordings are taken with a 35 mm photographic camera and are analyzed by a fully digital evaluation system (Willert 1995). The tracer particles used were the same as for LDV.

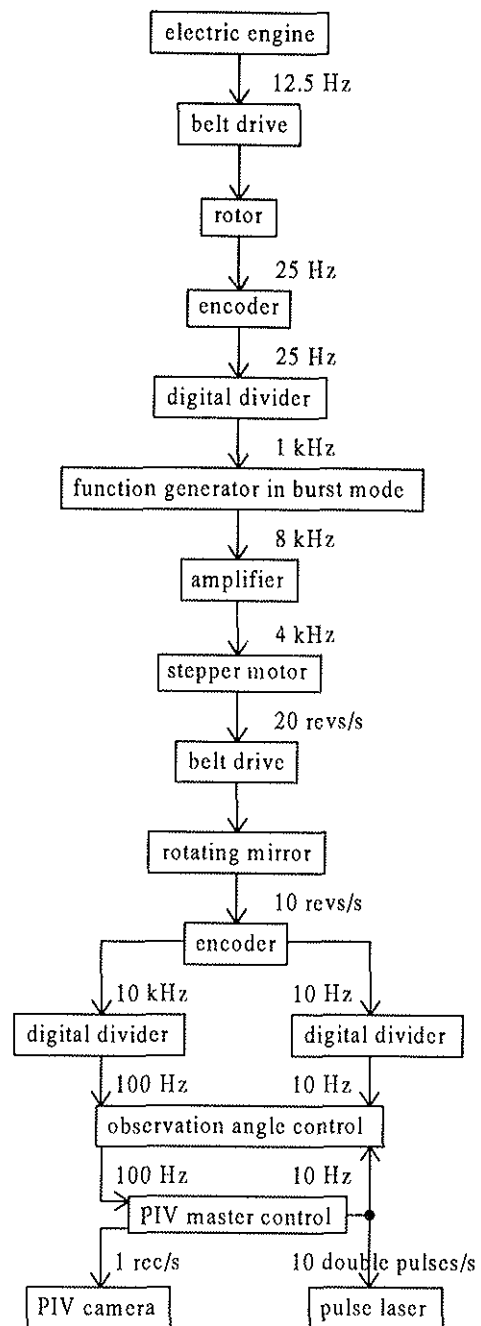


Figure 5: Synchronization scheme of PIV data acquisition.

Using the synchronization scheme shown in Figure 5 the recording of the PIV images could be performed phase locked with the motion of the helicopter rotor model. Therefore cycle-to-cycle variations of the flow field at the same azimuthal angle of the reference blade could be investigated by analysing up to 100 recordings each of which contained more than 2000 independent velocity vectors. However, only the two in-plane components of the velocity vectors could be measured by means of the photographic PIV system. Examples of fully digital, non-

photographic 2D-PIV measurements performed during the same measuring campaign are presented by Willert et al. (1996).

LDV results

In Figure 6 the tangential velocity profile of the tip vortex at $\psi = 0^\circ$ is shown along a line through the vortex center. For the measurement of the profile, the resolution was adapted to the extension of the vortex to be able to resolve the flow field gradients. From this data the vortex core diameter has been estimated to be 4.8 mm, respectively 8.9 % of the blade chord, and a maximum tangential velocity of 18 m/s, corresponding to $V_{tan} / U_\infty = 0.21$, when referenced to the free stream velocity.

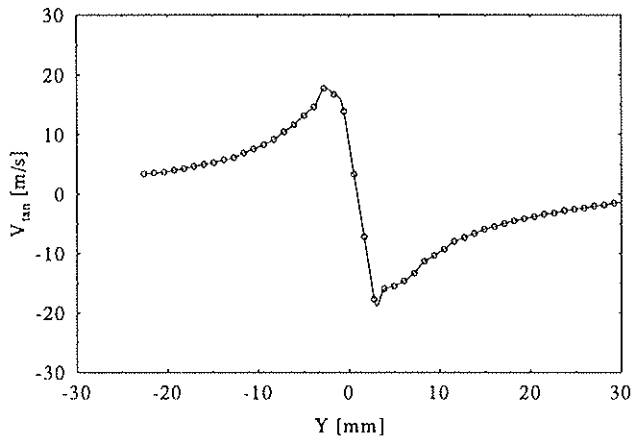


Figure 6: Tangential velocities along a line through the vortex center obtained by 3D-LDV.

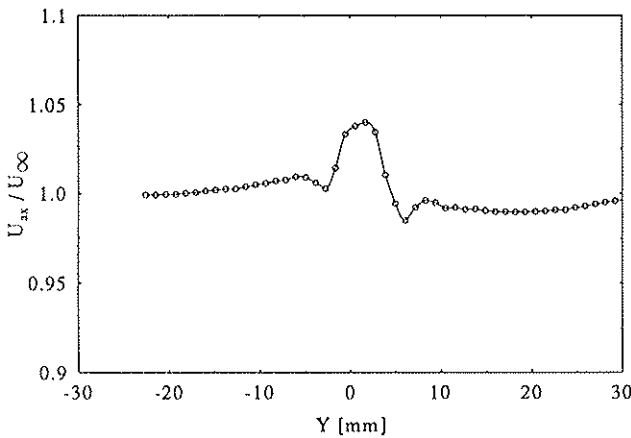


Figure 7: Axial velocities along a line through the vortex center obtained by 3D-LDV.

Figure 7 depicts the axial velocity profile of the tip vortex along the same line through the vortex center as for the tangential velocity profile given in Figure 6. For the axial velocity component there is an increase in velocity of 4 percent to $U_{ax} / U_\infty = 1.04$.

As shown in Figure 8, LDV measurements in a conditional sampling mode were collected in a plane perpendicular to the free stream velocity at the advancing

blade at an azimuthal angle of $\psi \approx 90^\circ$. This yielded in a three dimensional measurement grid, with the two coordinates obtained from traversing the LDV and the third coordinate derived from the transformation from time resolved velocity data to spatial velocity data. Thus, associated with each of these grid points is a local three dimensional velocity vector. The measurement plane 0.2 chord length behind the blade tip is shown in Figure 8 together with the locations of the tip vortices as predicted after the analysis of flow visualization data as obtained by Müller and Staufienbiel (1987). The origin of the coordinates was set to the point of intersection of the tip path of the blade (without aerodynamic load) and the observation area. The displacement of the tip path under load condition as measured by the position monitoring system was $Y = 10$ mm. By taking three dimensional velocity data at each grid point for a time of 1.75 ms, corresponding to an angular window of $\Delta\psi = 10^\circ$, leads, with a resolution of 0.5° , to a number of 20 measuring planes behind the rotor blade.

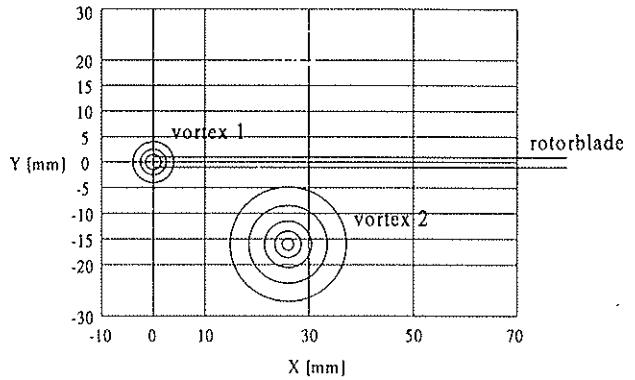


Figure 8: Measurement grid and expected position of vortices.

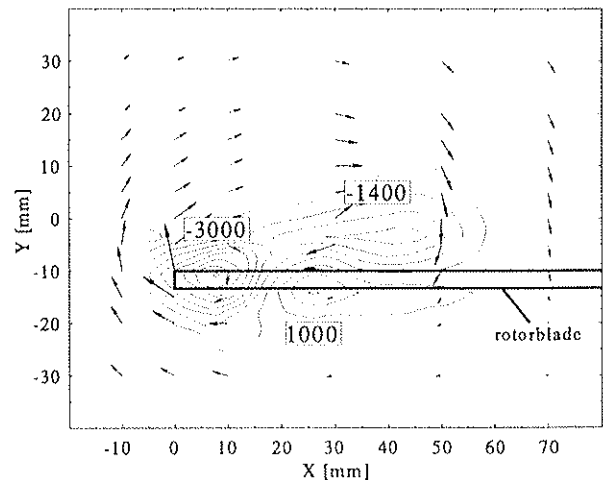


Figure 9: Velocity vector plot (2D) in a plane 0.2 chord length behind the blade tip as measured by LDV. The vorticity contours were obtained from the velocity data using finite differencing.

First, vector plots were computed from velocity data to give a general impression of the flow velocity field. Figure 9 clearly shows the vortex locations inside the measurement grid. At this azimuthal position a vortex can be observed, which has just been generated (age ≈ 0 ms, position corrected by the tip displacement $X = 5$ mm, $Y = 2.5$ mm). The vortex generated by the 90° advancing blade (age ≈ 10 ms, position corrected by the tip displacement $X = 40$ mm, $Y = 5$ mm) was located closer to the reference blade than expected (see also Fig. 9). Due to the location of the vortex generated by the advancing blade an interaction with the blade occurs, which results in an additional vortex of opposite rotational direction ($X = 25$ mm, $Y = -15$ mm). Since there was only little time elapsed between the generation of the tip vortices and their measurement (max. 10 ms) the cycle-to-cycle variations can be expected to be small.

From each of the 20 planes the maximum of vorticity of the newly generated blade tip vortex can be derived. This will give information on the temporal development. Due to conditional sampling also 10 additional planes in advance of the rotor blade are available, which include the information of the maximum vorticity of the 90 degree old vortex. Figure 10 shows the temporal development of the maximum vorticity of the blade tip vortex from $t = 0$ ms up to $t = 12$ ms. The vortex formation (I) can be described by a second order polynome, while its strenght decreases inversely proportional to its age, i.e. $1/t$ (II).

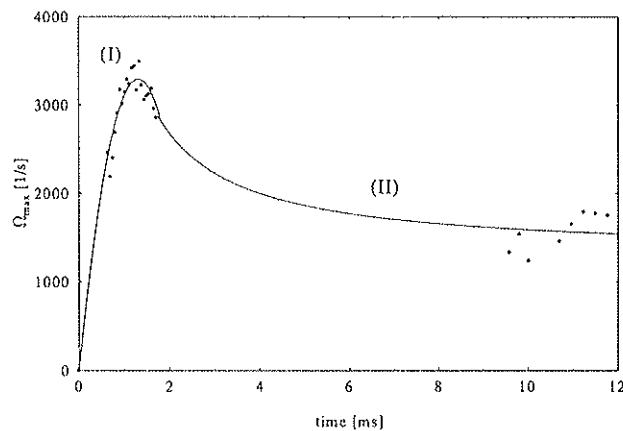


Figure 10: Temporal development of maximum vorticity of the blade tip vortex as measured by LDV.

PIV results

PIV measurements of orthogonal blade vortex interaction (position B) were taken at an azimuthal angle of $\psi \approx 90^\circ$ again on the advancing blade side. The observation area was nearly parallel to the trailing edge of the blade and orthogonal to the axis of the vortices. Figures 11a,b show two different instantaneous velocity vector fields from a set of 100 PIV recordings obtained at this angle. The origin was fixed to the tip of the trailing edge of the blade as it passed through the image plane with full aerodynamic load. Figure 11c is the velocity field obtained by averaging all 100 PIV data sets, and below (Fig. 11d) an estimate for the mean out-of-plane vorticity

component is given. The tip vortex (A), which has just been generated (age ≈ 0 ms), was located at $Y = 7.5$ mm, $Y = 2.5$ mm. A tip vortex (B) previously generated by the 90° advancing blade (age ≈ 10 ms), is now located at $X = 22$ mm, $Y = 25$ mm.

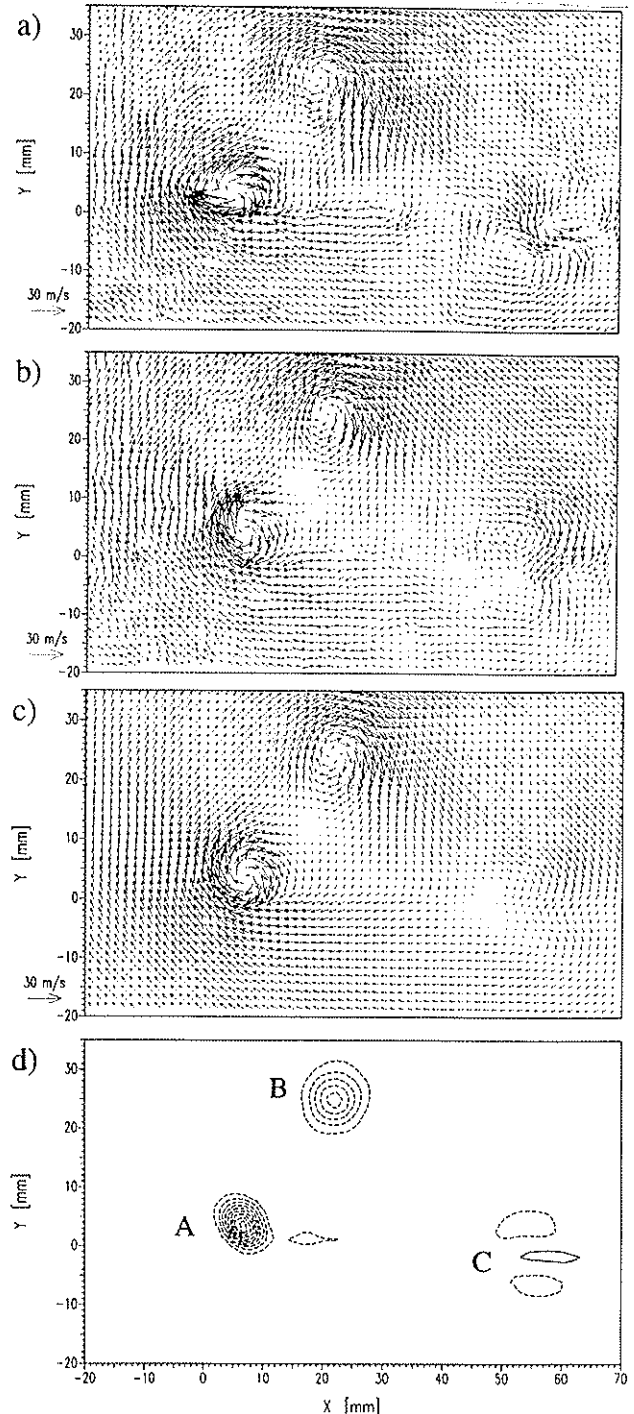


Figure 11: Two examples (a,b) of 100 instantaneous velocity vector fields as obtained by PIV at $\psi \approx 90^\circ$. Below (c) the averaged velocity field and (d) the corresponding vorticity estimate, ω_z , is shown. (Contour levels spaced at $1000/s$, dashed contours indicate negative values). Only portions of the 210 mm by 150 mm fields are shown for clarity.

The cycle-to-cycle variations of these two vortices were small enough such that they are properly resolved in the average velocity field. Close inspection of Figures 11a and 11b does however show some variations in the shape of the vortices. Also, a third vortex structure (C), generated by the 180° advancing blade, can be observed. As this vortex intersects the rotor plane at the same time the blade intersects the image plane, it is sliced by the blade (i.e. orthogonal BVI) such that only its remnants can be observed in the velocity field of Figure 11.

Due to small cycle-to-cycle variations this third vortex is sliced differently each time which results in the structure to be essentially lost in the averaged velocity field (Figure 11c).

In Figure 12 the tangential velocity profile of a tip vortex (age ≈ 0 ms) from a single PIV velocity data set has been plotted along a line through the vortex center.

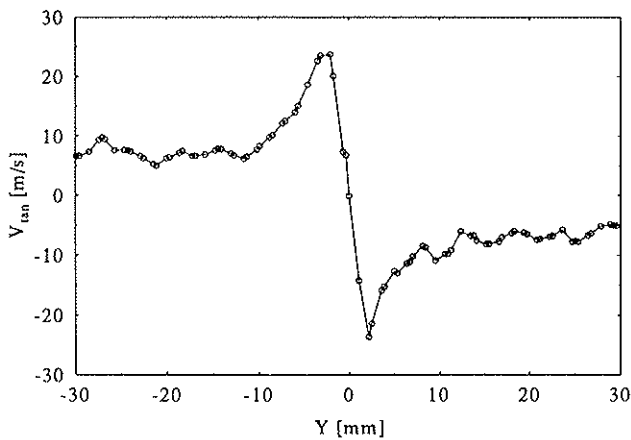


Figure 12: Tangential velocity along a line through the vortex center as obtained by a single PIV recording.

From these data the vortex core diameter has been estimated to be 7.4% of the blade chord, compared to 8.9% by the LDV method. The maximum tangential velocities (± 24 m/s) are 30% higher than those obtained by LDV (± 18 m/s). This discrepancy indicates the result of the averaging nature of the LDV method.

To investigate the uncertainty occurring by averaging the velocity field, the data of a number of instantaneous velocity vector fields (fig. 11 a,b) have been averaged. By this way, the amount of decreasing maximum tangential velocity and increasing vortex core size due to the averaging process can also be determined.

Figure 13 shows the tangential velocity profile along a line through the vortex center obtained by a spatial average over 36 PIV recordings. The maximum tangential velocity has been estimated to be ± 19 m/s and the vortex core size is 10.1 % of the blade chord. The maximum tangential velocity and the vortex core size are in the range of the results derived from the LDV data.

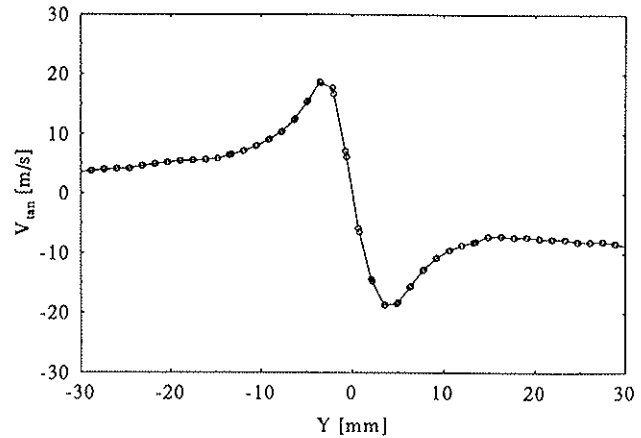


Figure 13: Tangential velocity along a line through the vortex center as obtained by an average over 36 PIV recordings.

In analogy to the available LDV data, the calculation of the temporal development of the maximum vorticity for the newly generated tip vortex can be performed. In this regard PIV recordings were obtained at different azimuthal positions of the rotor blade. From these the maximum vorticity in relation to the rotor azimuth was derived

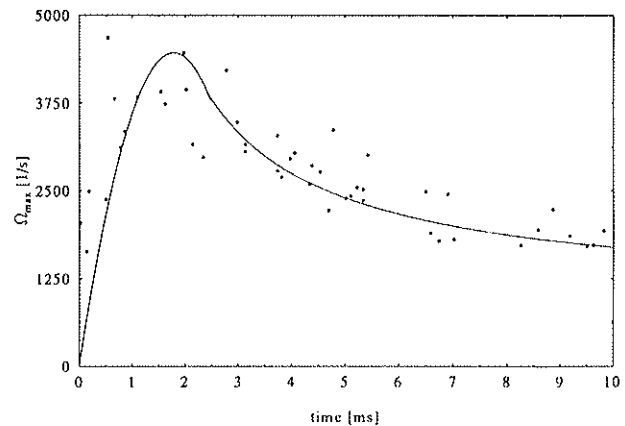


Figure 14: Temporal development of maximum vorticity of the blade tip vortex as measured by PIV.

Similar to the results derived from the LDV measurements, the roll up process can be described by a second order polynome, while the vortex dissipation is governed again by a $1/t$ dependence.

Discussion

The 3D-LDV measurements yielded fundamental results concerning the structure of the blade tip vortices. In addition to geometric parameters like location of the vortex relative to the rotor plane and orientation of the vortex axis in space, the vortex core size, axial velocity, vortex strength, and vorticity distribution had been derived. Although blade motion and local velocity had

been measured simultaneously, phase averaging and the rearrangement of the pointwise measured velocity data to form a complete velocity field causes some problems. Aperiodic flow phenomena, even of small amplitudes, can lead to the loss of cycle-to-cycle variation and thereby underestimate the actual vortex strength, and overestimate the core size of the vortex.

However, recent LDV measurements in large aerodynamic facilities show that 3D-LDV data of high quality can be obtained with good spatial resolution (Spletstößer et al. 1995).

But also in spite of the difficult experimental conditions high quality PIV data were obtained with sufficient spatial resolution. Compared to LDV measurements the time needed for data acquisition can be considerably decreased. A specially developed synchronization scheme allowed the capture of instantaneous flow field measurements at exactly the same phase angle of the rotor revolution and therefore the study of aperiodic features of the flow. Also with PIV the location of the vortex relative to the rotor plane, vortex core radius, convection speed, vortex strength and vorticity could be measured. However since conventional PIV measures only two velocity components, data, like the orientation of the vortex axis in space and axial velocity of a vortex, cannot be derived without changing the viewing direction. In future, using a second camera in stereoscopic arrangement would allow the measurement of all three velocity components without averaging data of different cycles.

From the comparison of the LDV and PIV data the differences in averaging and instantaneous data acquisition can be illustrated. By averaging a number of momentaneous PIV records a similar results for the LDA results is obtained especially regarding the vortex core size and the maximum tangential velocity. The temporal development of vortex formation and its dissipation can be obtained from both the LDV and PIV results and can be described by the analytical functions.

Literature

- B.M.J. Beesten
"Nichtplanare Rotorblattspitzen im Hubschraubervorwärtsflug"
Doctoral thesis, RWTH-Aachen, 1994.
- C.L. Burley, H.E. Jones, M.A. Marcolini,
W.R. Spletstößer
"Directivity and prediction of low frequency rotor noise"
AIAA 91-0592, Aerospace Science Meeting, Reno, USA
1991.
- F.X. Cardonne, J.L. Lautenschläger, M.J. Silva
"An experimental study of rotor-vortex interaction"
AIAA 88-0045, Aerospace Science Meeting, Reno, USA
1988.

K. Ehrenfried, G.E.A. Meier, F. Obermeier
"Sound produced by vortex-airfoil interaction"
Proc. of the 17th European Rotorcraft Forum, paper 63,
Berlin, Germany 1991.

J. Kompenhans, M. Raffel, A. Vogt, M. Fischer, B.
Bretthauer, H. Vollmers, B. Stasicki
"Investigation of Unsteady Flow Fields in Wind Tunnels
at High Flow Velocities by Means of Particle Image
Velocimetry"
Proc. of the 2nd International Conference on
Experimental Fluid Mechanics *ICEFM*, Ed. M. Onorato,
Levrotto & Bella, pp. 90-102, Turin, Italy 1994.

M.V. Lowson
"Progress towards quieter civil helicopters"
Proc. of the 17th European Rotorcraft Forum, paper 59,
Berlin, Germany 1991.

U. Seelhorst, K.A. Bütetfisch, K.H. Sauerland
"Three component Laser Doppler Velocimeter
development for large wind tunnels"
ICIASF '93 Record, paper 33, Saint Louis, France, 1993.

W.R. Spletstößer, K.J. Schultz, R.M. Martin
"Rotor blade-vortex interaction impulsive noise source
localization"
AIAA Journal, Vol. 28 No. 4, 593-600, 1990.

W.R. Spletstößer, R. Kube, W. Wagner, U. Seelhorst, A.
Boutier, F. Micheli, E. Mercker
"Key results from a higher harmonic control aeroacoustic
rotor test (HART) in the German-Dutch wind tunnel"
Proc. of the 21th European Rotorcraft Forum, St.
Petersburg, Russia, 1995.

C.E. Willert
"The fully digital evaluation of photographic PIV
recordings"
to appear in *Applied Scientific Research*, 1996.

C.E. Willert, M. Raffel, B. Stasicki, J. Kompenhans
"High-speed digital video camera systems and related
software for application of PIV in wind tunnel flows".
8. Int. Symp. on Appl. of Laser Techniques to Fluid
Mech., Lisbon, Portugal, 1996.

Acknowledgement

The scientific and technical support given by Prof. Neuwerth, Dr. Beesten, Dr. Gitek, and the team of the RWTH-Aachen low-speed wind tunnel is greatly appreciated.